Filtering schemes in the quantum-classical Liouville approach to nonadiabatic dynamics

Daniel A. Uken
School of Chemistry and Physics, University of KwaZulu-Natal, Private Bag X01, Scottsville 3209 Pietermaritzburg, South Africa

Alessandro Sergi
School of Chemistry and Physics, University of KwaZulu-Natal, Private Bag X01, Scottsville 3209 Pietermaritzburg, South Africa and National Institute for Theoretical Physics (NITheP), KwaZulu-Natal, South Africa

Francesco Petruccione
School of Chemistry and Physics and National Institute for Theoretical Physics, University of KwaZulu-Natal, Westville Campus, Private Bag X54001, Durban 4000, South Africa and National Institute for Theoretical Physics (NITheP), KwaZulu-Natal, South Africa

(Received 21 June 2013; published 4 September 2013)

We study a number of filtering schemes for the reduction of the statistical error in nonadiabatic calculations by means of the quantum-classical Liouville equation. In particular, we focus on a scheme based on setting a threshold value on the sampling weights, so that when the threshold is overcome the value of the weight is reset, and on another approach which prunes the ensemble of the allowed nonadiabatic transitions according to a generalized sampling probability. Both methods have advantages and drawbacks, however, their combination drastically improves the performance of an algorithm known as the sequential short-time step propagation [MacKernan *et al.*, J. Phys: Condens. Matter **14**, 9069 (2002)], which is derived from a simple first order expansion of the quantum-classical propagator. Such an algorithm together with the combined filtering procedures produce results that compare very well with those obtained by means of numerically accurate path integral quantum calculations for the spin-boson model, even for intermediate and strong coupling regimes.

DOI: 10.1103/PhysRevE.88.033301 PACS number(s): 05.10.−a, 03.65.−w, 05.30.−d

I. INTRODUCTION

In the field of condensed matter, many systems can be modeled using a quantum subsystem coupled to a classical bath. When energy is free to be exchanged between the subsystem and the bath, the resulting dynamics is known to be nonadiabatic. This type of dynamics is very difficult to simulate due to the quantum back-reaction of the subsystem onto the bath [1–5]. A number of numerical methods have been proposed for the calculation of nonadiabatic dynamics on a computer, the most common of which are so-called surface hopping schemes [6–12]. More recently, an approach based on the quantum-classical Liouville equation has been applied with success to condensed matter systems [13–19]. This approach allows one to construct a proper formulation of the statistical mechanics of quantum-classical systems [20,21] which can also be generalized to situations where the bath follows a non-Hamiltonian dynamics [22,23].

A simple and efficient algorithm suited for the computer simulation of the quantum-classical Liouville equation is the sequential short-time propagation (SSTP) algorithm [24]. The SSTP algorithm is based on a first order expansion in time of the Dyson form of the quantum-classical propagator and, when combined with the momentum-jump approximation [25,26], leads to a representation of nonadiabatic dynamics in terms of piecewise adiabatic trajectories of the bath coordinates, interspersed with stochastic transitions between the energy levels of the subsystem. Despite the similarities to a recently introduced scheme based on a Trotter decomposition of the quantum-classical propagator [27], the basic version of the SSTP algorithm is not as stable at long times and it also displays problems in the region of intermediate and strong coupling to the bath, as illustrated by the results of calculations on the spin-boson model [25,28,29]. The growth of the statistical error in time can be mitigated by means of filtering schemes. One such scheme [30] is essentially based on establishing a cutting threshold of the observable when it becomes too large because of the accumulation in time of the sampling weight. Such a scheme will be referred to in the following as the observable-cutting scheme. More recently, another filtering algorithm, which is based on a generalized sampling of nonadiabatic transitions, has been proposed. Such an algorithm has been proven to dramatically reduce the statistical error at long time [28,29]. This other scheme will be called in this paper as the transition-filtering scheme.

In this work, we use the SSTP algorithm to integrate the quantum-classical Liouville equation for the spin-boson model and perform a comparison of the performances of the two filtering schemes discussed above. The main result of this paper is that the SSTP algorithm used in conjunction with the combination of the observable-cutting and the transition-filtering schemes performs as well as the Trotter algorithm also in the intermediate and strong coupling regimes. This result is desirable since the SSTP algorithm is easier to implement than its Trotter counterpart, especially when the number of quantum states greater than two must be considered. This promises to be advantageous when studying quantum systems which are more complex than the spin-boson model.

The structure of the paper is as follows. Section II sketches the derivation of the quantum-classical Liouville equation and its representation in the adiabatic basis. In Sec. III, the basic version of the SSTP algorithm is illustrated together with the observable-cutting and the transition-filtering schemes. In the same section, the combined filtering scheme is introduced. Section IV discusses the results of the numerical calculations

on the dynamics of the spin-boson model using the various filtering schemes. Finally, our conclusions are given in Sec. V.

II. QUANTUM-CLASSICAL LIOUVILLE EQUATION

Let us consider a nonrelativistic system that is defined by the following Hamiltonian operator:

$$\hat{H} = \hat{H}_{\rm S} + \hat{H}_{\rm B} + \hat{H}_{\rm SB}\,, \tag{1}$$

where S, B, and SB are subscripts denoting the subsystem, bath, and the coupling, respectively. The Heisenberg equation of motion for an arbitrary operator $\hat{A}$ can be written in symplectic form as [22]

$$\frac{\partial}{\partial t}\hat{A} = \frac{i}{\hbar}[\,\hat{H}\;\hat{A}\,]\mathcal{B}^c\begin{bmatrix}\hat{H}\\ \hat{A}\end{bmatrix}, \tag{2}$$

where the symplectic matrix [31] $\mathcal{B}^c$ is given by

$$\mathcal{B}^c = \begin{bmatrix}0 & 1\\ -1 & 0\end{bmatrix}. \tag{3}$$

It is assumed that the Hamiltonian of the bath depends on a pair of canonically conjugate operators $\hat{X} = (\hat{R},\hat{P})$, and that the coupling Hamiltonian $\hat{H}_{\rm SB}$ depends only on $\hat{R}$ and not $\hat{P}$. The partial Wigner transform of the operator $\hat{A}$ over the bath coordinates is

$$\hat{A}_{\rm W}(X) = \int dz\, e^{iPz/\hbar}\left\langle R - \frac{z}{2}\middle|\hat{A}\middle|R + \frac{z}{2}\right\rangle. \tag{4}$$

The partial Wigner transform of the density matrix $\hat{\rho}$ of the system described by the Hamiltonian in Eq. (1) is

$$\hat{\rho}_{\rm W}(X) = \frac{1}{(2\pi\hbar)^{3N}}\int dz\, e^{iPz/\hbar}\left\langle R - \frac{z}{2}\middle|\hat{\rho}\middle|R + \frac{z}{2}\right\rangle, \tag{5}$$

where $X = (R,P)$ are now no longer operators but canonically conjugate classical phase-space variables. The partial Wigner transform of the Heisenberg equation of motion can be written in matrix form upon introducing the antisymmetric matrix operator $\mathcal{D}$ given by [22]

$$\mathcal{D} = \begin{bmatrix}0 & e^{\frac{i\hbar}{2}\overleftarrow{\partial}_k\mathcal{B}^c_{kj}\overrightarrow{\partial}_j}\\ -e^{\frac{i\hbar}{2}\overleftarrow{\partial}_k\mathcal{B}^c_{kj}\overrightarrow{\partial}_j} & 0\end{bmatrix}. \tag{6}$$

The symbols $\overleftarrow{\partial}_k = \overleftarrow{\partial}/\partial X_k$ and $\overrightarrow{\partial}_k = \overrightarrow{\partial}/\partial X_k$ denote the operators of derivation with respect to the phase-space coordinates acting to the left and right, respectively. The summation over repeated indices must be understood here and in the following. The partially Wigner-transformed Hamiltonian can be written as

$$\hat{H}_{\rm W}(X) = \hat{H}_{\rm S} + H_{\rm W,B}(X) + \hat{H}_{\rm W,SB}(R), \tag{7}$$

where we have assumed that the bath dependence of the coupling terms is on positions only:

$$\hat{H}_{\rm W,SB} = V_{\rm B}(R)\otimes\hat{H}'_{\rm S}, \tag{8}$$

where $H'_{\rm S}$ acts only in the Hilbert space of the subsystem. The above representation is equivalent to the Heisenberg representation, but in general calculations are difficult to perform. However, in many instances a quantum-classical approximation can be taken by means of a linear expansion of the exponential terms in the $\mathcal{D}$ matrix, giving

$$\mathcal{D}_{lin} = \begin{bmatrix}0 & 1 + \frac{i\hbar}{2}\overleftarrow{\partial}_k\mathcal{B}^c_{kj}\overrightarrow{\partial}_j\\ -1 - \frac{i\hbar}{2}\overleftarrow{\partial}_k\mathcal{B}^c_{kj}\overrightarrow{\partial}_j & 0\end{bmatrix}. \tag{9}$$

This allows one to write the quantum-classical Liouville equation as

$$\frac{\partial}{\partial t}\hat{A}(X,t) = \frac{i}{\hbar}[\,\hat{H}_{\rm W}(X)\;\hat{A}_{\rm W}(X,t)\,]\mathcal{D}_{lin}\begin{bmatrix}\hat{H}_{\rm W}(X)\\ \hat{A}_{\rm W}(X,t)\end{bmatrix}. \tag{10}$$

When $V_{\rm B}(R)$ is linear in R and $H_{\rm W,B}$ is quadratic in the bath coordinates, the linear expansion is exact ($\mathcal{D}_{lin} = \mathcal{D}$) and quantum-classical dynamics is equivalent to full quantum dynamics.

In order to perform calculations, Eq. (10) must be represented in a basis. The adiabatic basis leads naturally to a splitting of nonadiabatic and adiabatic terms, which is ideal for surface-hopping algorithms. To this end, the partially Wigner-transformed Hamiltonian in Eq. (7) can be rewritten as $\hat{H}_{\rm W} = (P^2/2M) + \hat{h}(R)$, so that the kinetic energy of the bath (represented in phase space) is separated from the rest of the energy terms that define the adiabatic Hamiltonian $\hat{h}(R)$. The adiabatic basis is defined as the solution to the eigenvalue equation

$$\hat{h}(R)|\alpha;R\rangle = E_\alpha(R)|\alpha;R\rangle. \tag{11}$$

In this basis, the quantum-classical evolution takes the form

$$A^{\alpha\alpha'}_{\rm W}(X,t) = \sum_{\beta\beta'}(e^{it\mathcal{L}})_{\alpha\alpha',\beta\beta'}A^{\beta\beta'}_{\rm W}(X), \tag{12}$$

where the quantum-classical Liouville operator [14] is given by

$$\begin{aligned} i\mathcal{L}_{\alpha\alpha',\beta\beta'} &= (i\omega_{\alpha\alpha'} + iL_{\alpha\alpha'})\delta_{\alpha\beta}\delta_{\alpha'\beta'} + J^{\rm MJ}_{\alpha\alpha',\beta\beta'}\\ &= i\mathcal{L}^0_{\alpha\alpha'}\delta_{\alpha\beta}\delta_{\alpha'\beta'} + J^{\rm MJ}_{\alpha\alpha',\beta\beta'}, \end{aligned} \tag{13}$$

where the MJ superscript denotes that we have used the momentum-jump approximation [25,26]. The Bohr frequency is defined as

$$\omega_{\alpha\alpha'}(R) = \frac{E_\alpha(R) - E_{\alpha'}(R)}{\hbar}, \tag{14}$$

and the classical-like Liouville operator for the bath degrees of freedom is given by

$$iL_{\alpha\alpha'} = \frac{P}{M}\frac{\partial}{\partial R} + \frac{1}{2}\left(F^\alpha_{\rm W} + F^{\alpha'}_{\rm W}\right)\frac{\partial}{\partial P}, \tag{15}$$

where $F^\alpha_{\rm W} = -\partial E_\alpha(R)/\partial R$ and $F^{\alpha'}_{\rm W} = -\partial E_{\alpha'}(R)/\partial R$ are the Hellman-Feynman forces for adiabatic energy surface E_α and $E_{\alpha'}$, respectively.

The operator $J^{\rm MJ}_{\alpha\alpha',\beta\beta'}$ is known as the transition operator in the momentum-jump approximation [25,26], and is responsible for the nonadiabatic transitions in the quantum subsystem and the accompanying changes in the bath momentum. It is given by

$$J^{\rm MJ}_{\alpha\alpha',\beta\beta'} = \mathcal{T}^{\rm MJ}_{\alpha\to\beta}\delta_{\alpha'\beta'} + \mathcal{T}^{*\rm MJ}_{\alpha'\to\beta'}\delta_{\alpha\beta}, \tag{16}$$

where

$$\mathcal{T}^{\mathrm{MJ}}_{\alpha\to\beta} = \frac{P}{M} d_{\alpha\beta}(R) \exp\left[\frac{1}{2}\frac{\Delta E_{\alpha\beta}(R) d_{\alpha\beta}(R)}{\frac{P}{M} d_{\alpha\beta}(R)} \frac{\partial}{\partial P}\right]. \tag{17}$$

In Eq. (17), the symbol $d_{\alpha\beta}(R) = \langle\alpha; R|(\partial/\partial R)|\beta; R\rangle$ denotes the coupling vector, while $\Delta E_{\alpha\beta}(R) = E_\alpha(R) - E_\beta(R)$ stands simply for the energy difference between the adiabatic eigenstates $|\alpha; R\rangle$ and $|\beta; R\rangle$. In the momentum-jump approximation, the back-reaction on the bath (i.e., the change to bath momenta) accompanying a nonadiabatic transition can be calculated analytically. If we consider an $\alpha \to \beta$ transition, the momentum-shift approximated J operator J^{MJ} produces a shift in the bath momenta P. This shift is defined as

$$P \to P' = P + \Delta^{\mathrm{MJ}}_{\alpha\beta} P, \tag{18}$$

where

$$\Delta^{\mathrm{MJ}}_{\alpha\beta} P = -(P\hat{d}_{\alpha\beta})\hat{d}_{\alpha\beta} + \hat{d}_{\alpha\beta}\,\mathrm{sgn}(P\hat{d}_{\alpha\beta})\sqrt{(P\hat{d}_{\alpha\beta})^2 + M\Delta E_{\alpha\beta}}\,. \tag{19}$$

The symbol $\hat{d}_{\alpha\beta} = d_{\alpha\beta}/\sqrt{d_{\alpha\beta}d_{\alpha\beta}}$ is the unit vector associated with the coupling vector in the multidimensional space of all the particle coordinates. Note that in the above, we have assumed that all the masses are the same, however, it is a simple matter to extend this to a system where the masses are different. If we expand the square root on the right-hand side of Eq. (19), we obtain the approximated form for the momentum-shift rule

$$\tilde{\Delta}^{\mathrm{MJ}}_{\alpha\beta} P = \frac{1}{2}\frac{\Delta E_{\alpha\beta}(R)}{\frac{P}{M}\hat{d}_{\alpha\beta}}\hat{d}_{\alpha\beta}. \tag{20}$$

Note that while the exact momentum-shift rule in Eq. (19) exactly conserves the energy, the approximated form in Eq. (20) does not. In our calculations, only the exact form of the momentum-shift rule was used.

III. FILTERING SCHEMES FOR THE SSTP ALGORITHM

The SSTP algorithm is derived upon considering the evolution along a quantum-classical trajectory given by the solution of Eq. (12) as a series of sequential small time steps τ. Hence, the short-time expression of the quantum-classical propagator $[\exp(i\tau\mathcal{L}^{\mathrm{MJ}})]_{\alpha\alpha',\beta\beta'}$ is approximated to linear order in time as

$$e^{i\tau\mathcal{L}^0_{\alpha\alpha'}}\left(\delta_{\alpha\beta}\delta_{\alpha'\beta'} + \tau J^{\mathrm{MJ}}_{\alpha\alpha',\beta\beta'}\right) = \mathcal{W}_{\alpha\alpha'}(\tau)e^{iL_{\alpha\alpha'}\tau} \times \left(\delta_{\alpha\beta}\delta_{\alpha'\beta'} + \tau J^{\mathrm{MJ}}_{\alpha\alpha',\beta\beta'}\right). \tag{21}$$

In Eq. (21), the phase factors $\mathcal{W}_{\alpha\alpha'}(\tau)$ are defined as $\mathcal{W}_{\alpha\alpha'}(\tau) = \exp[-i\int_0^\tau d\tau'\omega_{\alpha\alpha'}(\tau')]$, where the dependence on time of $\omega_{\alpha\alpha'}$, which is defined in Eq. (14), arises, in a Lagrangian point of view, from the time evolution of the coordinates of the bath R. In the limit $\tau \to 0$, the concatenation of the short-time steps exactly reproduces the Dyson integral expansion of the operator $\exp(i\tau\mathcal{L})_{\alpha\alpha',\beta\beta'}$ for finite times [24]. The computational evaluation of each single step τ can be evaluated upon considering the short-time propagator in Eq. (21) as a stochastic operator. The action of the transition operator $J^{\mathrm{MJ}}_{\alpha\alpha',\beta\beta'}$ is then sampled using a suitable transition probability. This transition probability is not uniquely fixed but has to be chosen following the criteria of physical reasonability and computational efficiency.

The transition probability is defined as the probability of a nonadiabatic transition occurring in a time interval τ. A basic choice for this probability is given by

$$\mathcal{P}^0_{\alpha\beta}(X,\tau) = \frac{\tau|\frac{P}{M}d_{\alpha\beta}(R)|}{1+\tau|\frac{P}{M}d_{\alpha\beta}(R)|}. \tag{22}$$

This transition probability then defines the probability of no transition occurring in the same time interval as

$$\mathcal{Q}^0_{\alpha\beta}(X,\tau) = 1 - \mathcal{P}^0_{\alpha\beta} = \frac{1}{1+\tau|\frac{P}{M}d_{\alpha\beta}(R)|} \tag{23}$$

when at time step t_j $(t_j - t_{j-1} = \tau)$ in the calculation the transition probability is sampled, and a transition occurs, the observable is multiplied by a factor $W_j = (\wp_{\alpha\beta})^{-1}\mathcal{W}_{\alpha\alpha'}(P/M)d_{\alpha\beta}(\mathcal{P}^0_{\alpha\beta})^{-1}$, where $\wp_{\alpha\beta}$ is the probability with which one selects state $|\beta; R\rangle$ being in state $|\alpha; R\rangle$. The $(P/M)d_{\alpha\beta}$ term originates from the action of the $J^{\mathrm{MJ}}_{\alpha\alpha',\beta\beta'}$ operator. If no transition occurs, then the weight at time t_j is defined as $W_j = \mathcal{W}_{\alpha\alpha'}(\mathcal{Q}_{\alpha\beta}{}^0)^{-1}$. In the SSTP algorithm, the total weight that multiplies the observable arises from the concatenation of all the weights W_j from $t = 0$ to the jth time step considered: $W = \prod_j W_j$. The growth of W with time and the fact that each nonadiabatic transition is accompanied by a shift of the momenta that can lead the bath to explore unstable regions of phase space cause an error in the calculation of the observable which also increases at longer times. We thus need to sample nonadiabatic transitions in such a way that minimizes this statistical error.

The first method for reducing statistical error tackles the problem directly. It is a simple but effective approach. As mentioned above, the magnitude of the weight, which is used to calculate the observable, grows with time and causes the value of the observable to grow, leading to large statistical error. Knowing this, we can introduce a threshold value κ_t which sets an upper bound to the magnitude of the weight. If at a time t_j in the calculation of a trajectory we have that the magnitude of the weight W becomes larger than κ_t, it is instead set to the value of κ_t. Mathematically, we can write this as

$$W = \begin{cases} W & \text{if} \quad |W| < \kappa_t, \\ \mathrm{sgn}(W)\kappa_t & \text{if} \quad |W| > \kappa_t. \end{cases} \tag{24}$$

Note that this cutting only affects the magnitude of the weight, the sgn remains the same. This cutting ensures that the weight can never grow to values where a single trajectory is having an overly large effect on the value of the observable. Consequently, we do not see the large statistical error in the result at longer times. Indeed, the logic behind the choice of κ_t is that of reducing the statistical error: a series of calculations has to be performed to discover the optimal choice of κ_t. While effective, however, this scheme does not have any physical basis, unlike the transition filtering scheme.

Another approach to the reduction of the statistical error has been recently proposed in Refs. [28,29]. Essentially, it is based

on filtering out those nonadiabatic transitions which would lead to too big a change in the momenta. In order to illustrate such an approach, it is useful to recall the form of the energy variation because of a nonadiabatic transition calculated using an approximate form of the momentum-shift rule:

$$\mathcal{E}_{\alpha\beta} = \frac{P'^2}{2M} + E_\alpha(R) - \left(\frac{P^2}{2M} + E_\beta(R)\right), \tag{25}$$

where $P' = P + \tilde{\Delta}^{\mathrm{MJ}}_{\alpha\beta} P$. Upon introducing the parameter $\kappa_{\mathcal{E}}$ and the weight $\omega(\kappa_{\mathcal{E}},\mathcal{E}_{\alpha\beta})$, one can define a generalized transition probability

$$\mathcal{P}^{EC}_{\alpha\beta}(X,\tau) = \frac{\tau|\frac{P}{M} d_{\alpha\beta}(R)|\omega(\kappa_{\mathcal{E}},\mathcal{E}_{\alpha\beta})}{1+\tau|\frac{P}{M} d_{\alpha\beta}(R)|\omega(\kappa_{\mathcal{E}},\mathcal{E}_{\alpha\beta})}. \tag{26}$$

This in turn defines the probability of no transition occurring as

$$\begin{aligned}\mathcal{Q}_{\alpha\beta}(X,\tau) &= 1 - \mathcal{P}^{EC}_{\alpha\beta} \\ &= \frac{1}{1+\tau|\frac{P}{M} d_{\alpha\beta}(R)|\omega(\kappa_{\mathcal{E}},\mathcal{E}_{\alpha\beta})}.\end{aligned} \tag{27}$$

The weight $\omega(\kappa_{\mathcal{E}},\mathcal{E}_{\alpha\beta})$ is defined as

$$\omega(\kappa_{\mathcal{E}},\mathcal{E}_{\alpha\beta}) = \begin{cases} 1 & \text{if } \mathcal{E}_{ab} \leqslant \kappa_{\mathcal{E}}, \\ 0 & \text{otherwise.} \end{cases} \tag{28}$$

The transition probabilities in Eqs. (26) and (27) allow one to control the amplitude of energy fluctuations that would be caused by an approximate momentum-shift rule through the use of the numerical parameter $\kappa_{\mathcal{E}}$. Whenever a nonadiabatic transition would cause a virtual energy fluctuation that is larger than $\kappa_{\mathcal{E}}$, the transition probability becomes zero, and no transition can occur. As in the case of κ_{t} in the observable-cutting scheme, the choice of $\kappa_{\mathcal{E}}$ in the transition-filtering scheme is dictated by the rationale of reducing the statistical error of the results of the calculations. This generalization of the basic sampling scheme allows nonadiabatic transitions to occur only in regions where the approximate momentum-shift rule causes small virtual variation of the energy of the system: this happens when the change in the momentum is not too big. Such a scheme has been proven numerically to be very efficient in reducing statistical error at long times [28,29]. In the transition sampling scheme defined by Eqs. (25)–(28), the use of the virtual energy variation in Eq. (25), as arising from the approximated momentum-shift rule in Eq. (20) which is not used in the actual calculation, must be considered as a computational trick in order to select nonadiabatic transitions that do not lead the system to an unstable region of phase space because of too great a change in the bath coordinates's momenta. As a matter of fact, the approximated momentum-shift rule in Eq. (20) coincides numerically with the exact momentum-shift rule in Eq. (19) for small changes of the momenta.

Since each of the above filtering techniques approach the statistical error problem from different angles, it is interesting to combine them within a single simulation algorithm. According to such an idea, in each simulation, the nonadiabatic transitions are filtered according to the transition-filtering scheme, using the parameter $\kappa_{\mathcal{E}}$, in addition to the observable being cut when it grows too large, according to the parameter κ_{t}.

IV. NUMERICAL CALCULATIONS

Our numerical study was performed on the spin-boson model [32], which can be considered as a paradigmatic example for quantum dynamics [25] for which the adiabatic states are known exactly. For this system, there are also available accurate numerical results arising from the integration of its quantum dynamics by means of path integral techniques [33–38] and classical mapping approaches [39]. Such a system comprises a single spin coupled to a bath of harmonic oscillators. Since the bath is harmonic and the coupling to the spin is bilinear, the quantum-classical Liouville equation is formally identical, after the partial Wigner transform over the bath coordinate, to the Heisenberg equation of motion so that the quantum-classical dynamics of this model is exact, i.e., perfectly equivalent to its quantum dynamics. Using adimensional coordinates [24,25,27], the spin-boson Hamiltonian is given by defining the various terms in Eq. (7) as

$$\hat{H}_{\mathrm{S}} = -\Omega\hat{\sigma}_x, \tag{29}$$

$$H_{\mathrm{W,B}} = \sum_{i=1}^{N}\left(\frac{P_i^2}{2} + \frac{1}{2}\omega_i^2 R_i^2\right), \tag{30}$$

$$\hat{H}_{\mathrm{W,SB}} = -\sum_{i=1}^{N} c_i R_i \hat{\sigma}_z, \tag{31}$$

where $\hat{\sigma}_x$ and $\hat{\sigma}_z$ are the Pauli spin matrices and c_i are the coupling coefficients. These coefficients are determined by requiring that the system spectral density is Ohmic [36]. In adimensional units, they are defined as $c_j = \sqrt{\xi(\omega_0/\omega_c)}\omega_j$ where ξ is the Kondo parameter and ω_c the frequency characterizing the Ohmic spectral density and which provides the fundamental unit of measure for all the other quantities. The mode frequencies are defined as $\omega_j = -\ln(1 - j\omega_0/\omega_c)$ and the zeroth frequency is defined as $\omega_0 = \omega_c[1 - \exp(-\omega_{\max}/\omega_c)]/N$.

In simulations, we have set the spin in an excited state at $t = 0$, and the quantum harmonic modes are at thermal equilibrium, with no coupling before $t = 0$. After $t = 0$, the coupling is switched on, and we calculate the observable $\langle\hat{\sigma}_z(t)\rangle$, or population difference of the system. We have considered $n = 2$ nonadiabatic transitions per trajectory, as this was sufficient for the results to converge. Each simulation used a total of $N_{\mathrm{mcs}} = 10^5$ sampled phase-space points for the initial conditions. The integration time step was $dt = 0.1$ in dimensionless units.

Figures 1 and 2 give the results for weak coupling, with system parameters $\beta = 0.3$, $\xi = 0.007$, and $\Omega = \frac{1}{3}$. From Fig. 1, we see that both filtering techniques give results that agree well with the influence functional path integral calculations [36], however, the two results deviate from each other at longer times. For both cases, we can observe the growth of the statistical error at longer times, although it is relatively minimal for weak coupling. Figure 2 displays the weak coupling result for the combined filtering scheme. In this case we again see the excellent agreement with the influence functional results, but the error bars are smaller

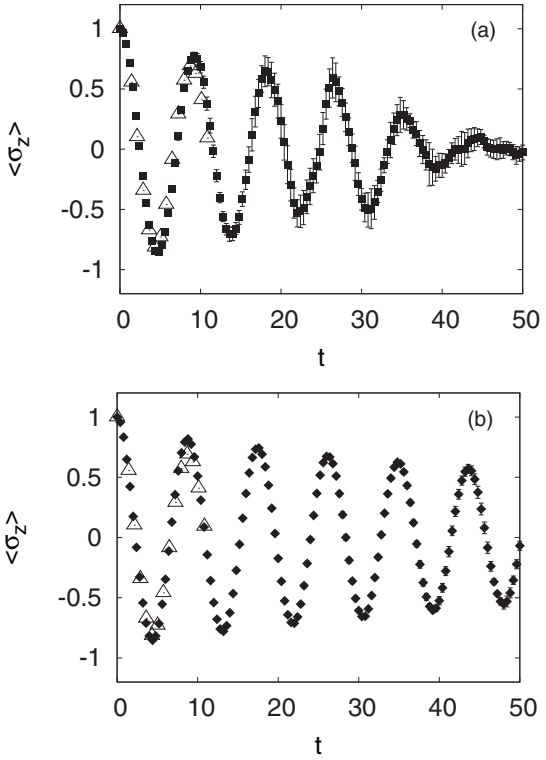

FIG. 1. Comparison of the SSTP with the observable-cutting (filled square, panel a) and the transition-filtering algorithm (filled diamond, panel b) to path integral quantum results (open triangle) from Refs. [33–35]. System parameters were $\beta = 0.3$, $\xi = 0.007$, $\Omega = \frac{1}{3}$, corresponding to weak coupling. The value of the threshold parameter for the observable cutting was $\kappa_t = 100.0$, and the value of the control parameter for the energy conserving filtering was $\kappa_\mathcal{E} = 0.005$. Two nonadiabatic transitions were included in the calculations.

than the points for the entire simulation time. Moreover, the calculation remains stable for longer times [28,29] than those obtained in previously published results.

Figures 3 and 4 show the results for mid-range coupling. The system parameters used were $\beta = 12.5$, $\xi = 0.09$, and

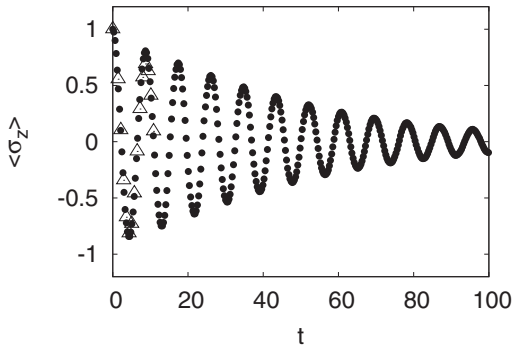

FIG. 2. Comparison of the SSTP with the combined filtering algorithm (filled circle) to path integral quantum results (open triangle) from Refs. [33–35]. System parameters were $\beta = 0.3$, $\xi = 0.007, \Omega = \frac{1}{3}$. The value of the threshold parameter was $\kappa_t = 1.5$, and the value of the energy conserving filtering control parameter was $\kappa_\mathcal{E} = 0.005$. Two non-adiabatic transitions were included in the calculations.

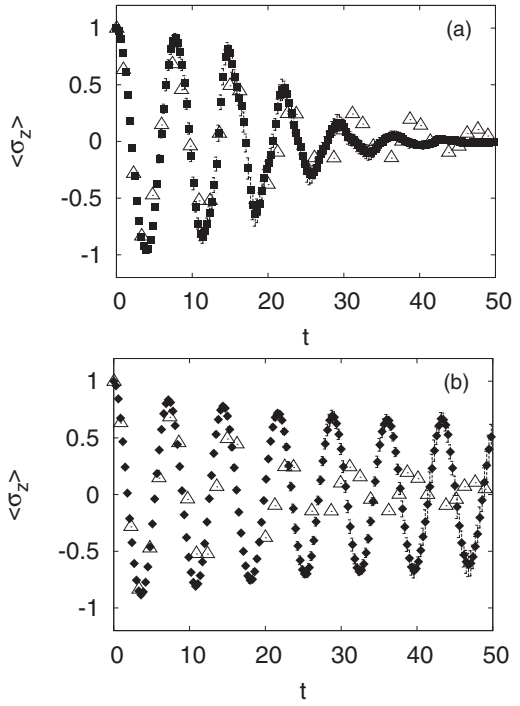

FIG. 3. Comparison of the SSTP with the observable-cutting (filled square, panel a) and the transition-filtering algorithm (filled diamond, panel b) to path integral quantum results (open triangle) from Ref. [36]. System parameters were $\beta = 12.5$, $\xi = 0.09$, $\Omega = 0.4$, corresponding to mid-range coupling. The value of the threshold parameter for the direct filtering was $\kappa_t = 50.0$, and the value of the control parameter was $\kappa_\mathcal{E} = 0.025$. Two nonadiabatic transitions were included in the calculations.

$\Omega = 0.4$. Figure 3 gives the comparison of the two filtering schemes. The results for both filtering schemes agree very well with the path integral quantum result from Ref. [36] up until approximately $t = 20$, but after this time the results deviate somewhat. In the case of the transition-sampling filter, we do not observe the damping that occurs in the path integral result: the oscillations remain large. For the observable-cutting scheme, however, we see the opposite.

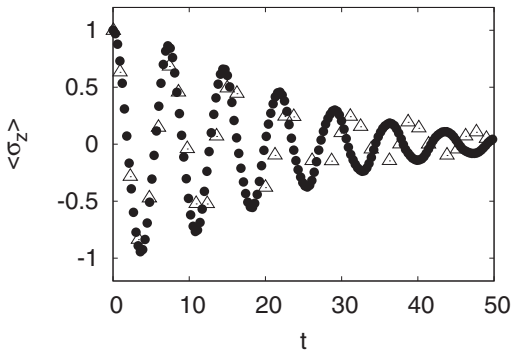

FIG. 4. Comparison of the SSTP with the combined filtering algorithm (filled circle) to path integral quantum results (open triangle) from Ref. [36]. System parameters were $\beta = 12.5, \xi = 0.09$, $\Omega = 0.4$. The value of the threshold parameter was $\kappa_t = 3.5$, and the value of the control parameter was $\kappa_\mathcal{E} = 0.05$. Two nonadiabatic transitions were included in the calculations.

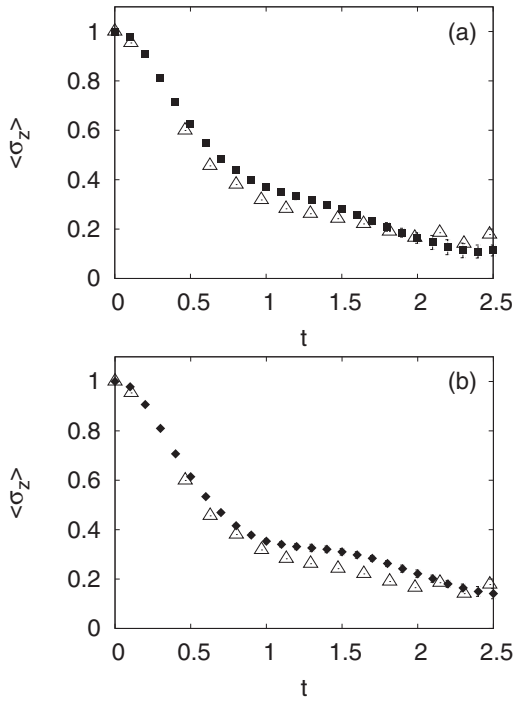

FIG. 5. Comparison of the SSTP with the observable-cutting (filled square, panel a) and the transition-filtering algorithm (filled diamond, panel b) to path integral quantum results (open triangle) from Ref. [38]. System parameters were $\beta = 0.25, \xi = 2.0, \Omega = 1.2$, corresponding to high coupling. The value of the bound parameter for the direct filtering was $\kappa_t = 50.0$, and the value of the control parameter was $\kappa_\mathcal{E} = 0.5$. Two nonadiabatic transitions were included in the calculations.

The observable-cutting filter damps the result too much at longer times, causing it to become zero. In Fig. 4, we have the result for the combined filtering scheme. We see a dramatic improvement over both the individual filtering scheme since the combined filter does not exhibit either of the problems observed above. The combined filtering result agrees far better with the path integral quantum result at longer times, with the error bars smaller than the points for the entire simulation time.

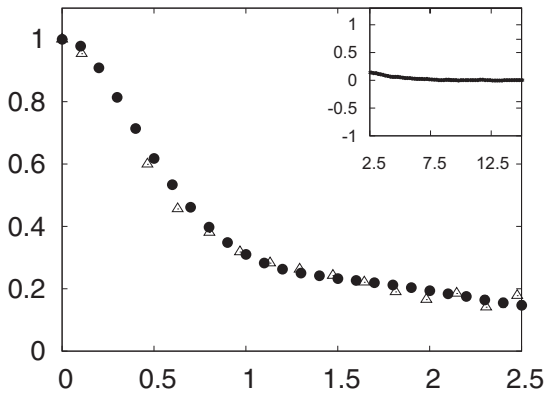

FIG. 6. Comparison of the SSTP with the combined filtering algorithm (filled circle) to path integral quantum results (open triangle) from Ref. [38]. System parameters were $\beta = 0.25, \xi = 2.0, \Omega = 1.2$. The value of the threshold parameter was $\kappa_t = 5.0$, and the value of the control parameter was $\kappa_\mathcal{E} = 1.0$. Two nonadiabatic transitions were included in the calculations.

In Figs. 5 and 6, the results for strong coupling are presented. For these results, we adopted the system parameters $\beta = 0.25$, $\xi = 2.0$, and $\Omega = 1.2$. From Fig. 5 we can see that the two filtering schemes are incapable of reproducing the quantum results of Ref. [38] at even short times. Although both schemes are successful at reducing the statistical error, we do see that the error bars become larger than the points at approximately $t = 2$. In Fig. 6, we show the result obtained with the combined filtering scheme for strong coupling. Again, the improvement is remarkable. In the main figure, an excellent agreement with the quantum result is illustrated, while the inset shows that the result can be extended to long times with statistical error remaining smaller than the points.

V. CONCLUSIONS

We have studied three different methods for reducing the statistical error when simulating the quantum-classical Liouville approach to nonadiabatic dynamics by means of the sequential short-time step algorithm [24]. The first two methods are the observable-cutting scheme (which uses the reset to threshold value for the statistical weights entering the definition of the observable) and the transition-filtering approach (which prunes the ensemble of allowed nonadiabatic transitions on the basis of a generalized sampling probability). We have used the spin-boson model as a paradigmatic example of quantum dynamics in a dissipative environment [32] and performed numerical calculations on the evolution in time of the state population difference of this model. The use of either scheme gives rise to results that have smaller statistical error than those obtained when using the basic sampling, and both filtering techniques are capable of producing results in good agreement with the numerically accurate path integral quantum results for short times, but only for the intermediate and weak coupling regimes. Although both schemes are an improvement over the basic sampling method in the SSTP algorithm, they are still unable to reproduce the numerically accurate path integral quantum results for strong coupling, and fail at longer times for intermediate coupling as well. Moreover, both schemes, when used in separation from the other, are not able to curb the increase of the statistical error at longer times.

Nevertheless, we have shown that the combination of these two filtering methods in a single scheme solves both of the problems encountered by the individual filtering schemes. This is the main result of this paper. Upon using the combined filtering scheme, we have produced results that not only have negligible statistical error for longer simulation time than that accessible in previously published calculations, but compare far more favorably with the numerically accurate path integral quantum results. The combined method is able to nearly perfectly reproduce the strong coupling results, whereas the individual schemes could not do this even at very short times. Our results are also as good as those obtained with the Trotter-based algorithm for the simulation of the quantum-classical Liouville equation [27]. However,

since the SSTP algorithm is easier to implement for systems which have a number of quantum states greater than two, our proposal of the combined filtering scheme promises to be advantageous for more complex numerical studies of nonadiabatic dynamics.

ACKNOWLEDGMENTS

This work is based upon research supported by the South African Research Chair Initiative of the Department of Science and Technology and the National Research Foundation.

[1] I. V. Aleksandrov, Z. Naturforsch., A: Phys. Sci. **36A**, 902 (1981).
[2] V. I. Gerasimenko, Theor. Math. Phys. **50**, 77 (1982).
[3] W. Boucher and J. Traschen, Phys. Rev. D **37**, 3522 (1988).
[4] W. Y. Zhang and R. Balescu, J. Plasma Phys. **40**, 199 (1988).
[5] R. Balescu and W. Y. Zhang, J. Plasma Phys. **40**, 215 (1988).
[6] J. C. Tully and R. K. Preston, J. Chem. Phys. **55**, 562 (1971).
[7] W. H. Miller and I. F. George, J. Chem. Phys. **56**, 5637 (1972).
[8] P. Pechukas, Phys. Rev. **181**, 166 (1969).
[9] P. Pechukas, Phys. Rev. **181**, 174 (1969).
[10] E. J. Heller, B. Segev, and A. V. Sergeev, J. Phys. Chem. B **106**, 8471 (2002).
[11] N. Shenvi, J. Chem. Phys. **130**, 124117 (2009).
[12] *Classical and Quantum Dynamics in the Condensed Phase Simulations*, edited by B. J. Berne, G. Ciccotti, and D. Coker (World Scientific, Singapore, 1998).
[13] C. C. Martens and J.-Y. Fang, J. Chem. Phys. **106**, 4918 (1997).
[14] R. Kapral and G. Ciccotti, J. Chem. Phys. **110**, 8919 (1999).
[15] I. Horenko, C. Salzmann, B. Schmidt, and C. Schutte, J. Chem. Phys. **117**, 11075 (2002).
[16] Q. Shi and E. Geva, J. Chem. Phys. **121**, 3393 (2004).
[17] A. Sergi, I. Sinayskiy, and F. Petruccione, Phys. Rev. A **80**, 012108 (2009).
[18] N. Rekik, C.-Yu Hsieh, H. Freedman, and G. Hanna, J. Chem. Phys. **138**, 144106 (2013).
[19] Qiang Shi and Eitan Geva, J. Chem. Phys. **131**, 034511 (2009).
[20] S. Nielsen, R. Kapral, and G. Ciccotti, J. Chem. Phys. **115**, 5805 (2001).
[21] A. Sergi, J. Chem. Phys. **124**, 024110 (2006).
[22] A. Sergi, Phys. Rev. E **72**, 066125 (2005).
[23] A. Sergi, J. Phys. A: Math. Theor. **40**, F347 (2007).
[24] D. MacKernan, R. Kapral, and G. Ciccotti, J. Phys.: Condens. Matter **14**, 9069 (2002).
[25] A. Sergi, D. Mac Kernan, G. Ciccotti, and R. Kapral, Theor. Chem. Acc. **110**, 49 (2003).
[26] R. Kapral and G. Ciccotti, in *Bridging Time Scales: Molecular Simulations for the Next Decade*, SIMU Conference 2001, edited by P. Nielaba, M. Mareschal, and G. Ciccotti (Springer, Berlin, 2003), p. 445.
[27] D. Mac Kernan, G. Ciccotti, and R. Kapral, J. Phys. Chem. B **112**, 424 (2008).
[28] A. Sergi and F. Petruccione, Phys. Rev. E **81**, 032101 (2010).
[29] D. A. Uken, A. Sergi, and F. Petruccione, Phys. Scr. T **143**, 014024 (2011).
[30] G. Hanna and R. Kapral, J. Chem. Phys. **122**, 244505 (2005).
[31] H. Goldstein, *Classical Mechanics* (Addison-Wesley, Reading, 1980).
[32] A. J. Leggett, S. Chakravarty, A. T. Dorsey, M. P. A. Fischer, A. Garg, and M. Zwerger, Rev. Mod. Phys. **59**, 1 (1987).
[33] K. Thompson and N. Makri, J. Chem. Phys. **110**, 1343 (1999).
[34] N. Makri, J. Phys. Chem. B **103**, 2823 (1999).
[35] N. Makri and K. Thompson, Chem. Phys. Lett. **291**, 101 (1998).
[36] D. E. Makarov and N. Makri, Chem. Phys. Lett. **221**, 482 (1994).
[37] R. Egger and C. H. Mak, Phys. Rev. B **50**, 15210 (1994).
[38] C. H. Mak and D. Chandler, Phys. Rev. A **44**, 2352 (1991).
[39] A. A. Golosov and D. R. Reichman, J. Chem. Phys. **114**, 1065 (2001).